Drought Assessment in Paddy Rice Fields Using Multi-temporal SAR Data of Sentinel-1: A Case Study in Tra Vinh Province

Tien Duy Pham, Diep Thi Hong Nguyen, and Can Trong Nguyen

Abstract This study presents an innovative approach to mapping rice cultivation patterns and assessing drought conditions in Tra Vinh province, Vietnam, using multi-temporal Synthetic Aperture Radar (SAR) data from the Sentinel-1 satellite and Vegetation Health Index (VHI) derived from Moderate Resolution Imaging Spectroradiometer (MODIS) data. The research was conducted over the period 2014–2021 and made use of the Google Earth Engine (GEE) cloud computing platform. The findings reveal a dominant prevalence of triple rice cropping, which occupies approximately 75% of the total rice cultivation area in the province. Further, there was a significant interannual variability in drought severity, with particularly severe conditions observed in 2015 and a resurgence in 2020/2021. Over the study period, there has been a concerning trend of an increasing area affected by mild and moderate drought conditions. The study highlights the potential of remote sensing techniques, particularly SAR data, in monitoring agricultural systems in tropical regions with frequent cloud cover. The results provide critical insights that can inform sustainable agricultural planning, water resource management, and climate change mitigation strategies in Tra Vinh province and similar rice-producing

T. D. Pham
Rural Development and Natural Resources, Faculty of Agriculture and Natural Resources, An Giang University, Long Xuyen, An Giang, Vietnam

Viet Nam National University, Ho Chi Minh City, Vietnam
e-mail: pdtien@agu.edu.vn

D. T. H. Nguyen (✉)
Department of Land Resources, College of Environment and Natural Resources, Can Tho University, Can Tho, Vietnam
e-mail: nthdiep@ctu.edu.vn

C. T. Nguyen
Environment Centre, Charles University, Dejvice, Czech Republic

W. Boonpook et al. (eds.), *Applied Geography and Geoinformatics for Sustainable Development*, Springer Geography,
https://doi.org/10.1007/978-3-031-84308-2_7

regions. Future research should consider integrating multi-sensor data sources for enhanced accuracy in rice crop classification and drought assessment.

Keywords Vegetation health index · Drought · Google earth engine · Tra Vinh province · Climate change

1 Introduction

In Vietnam, rice not only serves as the primary food source for over 100 million people but also significantly contributes to the country's food security and rural economy, constituting an indispensable component of its agricultural exports. Specifically, the Mekong River Delta (MRD) is one of Vietnam's key agricultural regions, with its rice cultivation area accounting for 54.2% of the country's total rice cultivation area. Beyond rice, the MRD also significantly contributes to the production of seafood and fruits, accounting for 86.3% and 64.7% of the total production, respectively [1].

Tra Vinh, a coastal province within the Mekong Delta, plays a significant role in Vietnam's rice production. However, Tra Vinh also faces significant challenges due to climate change, particularly drought, which affects rice productivity and yields. Therefore, monitoring changes in rice cultivation and assessing drought levels are essential to ensure food security and sustainable development for the province.

Over the last several years, remote sensing technology, which involves seeing the Earth from space, has greatly enhanced the ability to monitor the Earth's surface and its natural resources [2]. Numerous studies worldwide have employed this method. Huang [3] used Landsat data to examine changes in land cover in China, for example. In India, Kukunuri [4] used MODIS (Moderate Resolution Imaging Spectroradiometer) data to precisely categorize agricultural droughts. Liu [5] used MODIS data to create three catastrophe monitoring models in China.

In addition, remote sensing methods have been essential in the mapping of rice fields [6] and the monitoring of drought in different locations, especially in rice fields, by using various vegetation indices [7]. However, a common challenge with optical images is their susceptibility to hazy conditions. Researchers have explored various approaches to mitigate the effects of clouds [8–10], but continuous cloud cover poses a significant challenge in tropical monsoon areas like Vietnam, especially during the rainy period. Satellites like Sentinel-1 and COSMO-SkyMed use microwave remote sensing, which is largely unaffected by atmospheric conditions like fog, rain, snow, clouds, and smoke, unlike other forms of remote sensing. The level of impact may vary depending on the wavelength utilized. These satellites provide a great level of detail and accuracy in both space and time, making them well-suited for the mapping of rice fields [11, 12].

Despite these advancements, no study has utilized the Google Earth Engine (GEE) cloud computing platform and satellite data to map rice fields across the entire Tra Vinh Province. Similarly, no research has been conducted to develop

spatially distributed maps of vegetation indices to assess drought in this province. This study aims to investigate changes in rice cultivation patterns in Tra Vinh province over the 2014–2021 period and to evaluate the effectiveness of vegetation indices, Vegetation Condition Index (VCI), Thermal Condition Index (TCI), and Vegetation Health Index (VHI), in detecting and assessing drought conditions within the province's rice fields.

2 Study Area

Tra Vinh, a province strategically located in the Mekong Delta region, is blessed by nature with a 65-km-long coastline and a dense network of rivers. The province borders Ben Tre, Vinh Long, and Soc Trang, creating a diverse cultural and economic landscape. With an area of 2356 km^2, Tra Vinh consists of 1 city, 8 districts, and 80 communes. The province's population exceeds one million people, forming a diverse and cohesive community. The economy of Tra Vinh has developed multisectorally, focusing on areas such as agriculture, aquaculture, industry, and tourism. The advantages of geography and abundant resources have contributed to the socioeconomic development of the province in recent years [13] (Fig. 1).

Farmers in Tra Vinh province benefit from advantageous climate, water resources, and soil conditions, allowing them to grow rice multiple times per year. The distinct

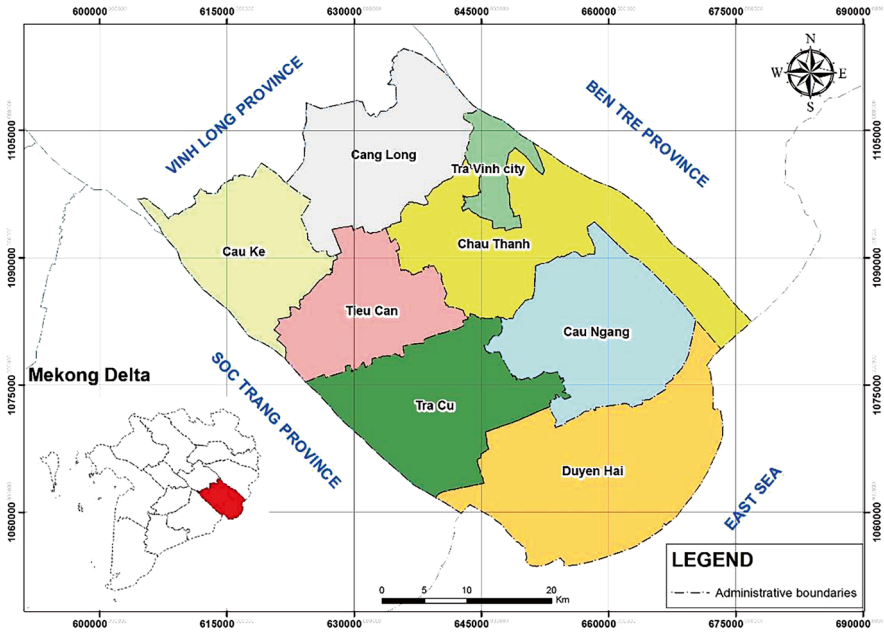

Fig. 1 Location map of the study area

Table 1 Summary of rice farming practices in Tra Vinh Province

Farming method	Seasons	Sowing schedule
Single-rice crop	Mua (traditional rice)	Mua period (July/August–Oct/Nov)
Double-rice crop	Dong Xuan (winter-spring) and He Thu (summer-autumn)	Dong Xuan (November–January), He Thu (May–June)
Triple-rice crop	Dong Xuan (winter-spring), He Thu (summer-autumn), Thu Dong (autumn-winter)	Dong Xuan (November–January), He Thu (May–June), Thu Dong (July–August)

Source: [14]

planting seasons are known as winter-spring (WS), summer-autumn (SA), and autumn-winter (AW). Of these seasons, the summer-autumn (SA) period generally results in the highest rice yields within the province. There's also the traditional rice season (Mua), where older rice varieties with extended growth cycles are used. While yields tend to be lower during this season, the rice produced is known for its exceptional quality.

In terms of rice farming practices in the province, there are three main systems: single-rice crop, double-rice crop, and triple-rice crop, each with distinct characteristics and outputs as detailed in Table 1.

3 Data and Methodology

The research utilized a detailed method combining Google Earth Engine (GEE) and ENVI software, as depicted in its flow chart (Fig. 2). The process involved nine key steps: collecting and processing field data, pre-processing Synthetic Aperture Radar (SAR) data, extracting mean values from this data, comparing and selecting SAR data polarization modes, masking non-rice cultivation areas, defining specific analysis parameters, selecting temporal features for in-depth temporal analysis, setting up decision rules for data analysis, and validating and mapping with classifiers. These steps enabled the extraction and mapping of geographic distributions of vegetation indicators, ensuring a comprehensive and accurate assessment of the research goals.

3.1 Field Data Processing

After completing the field work, the team manually converted the collected questionnaire data into digital format. To ensure clarity and consistency across the dataset, each rice plot was given a distinct column name, and a uniform row coding style was applied across all 100 charts. The process of digitizing the rice plots involved importing their GPS coordinates into Google Earth. In this phase, the team visually

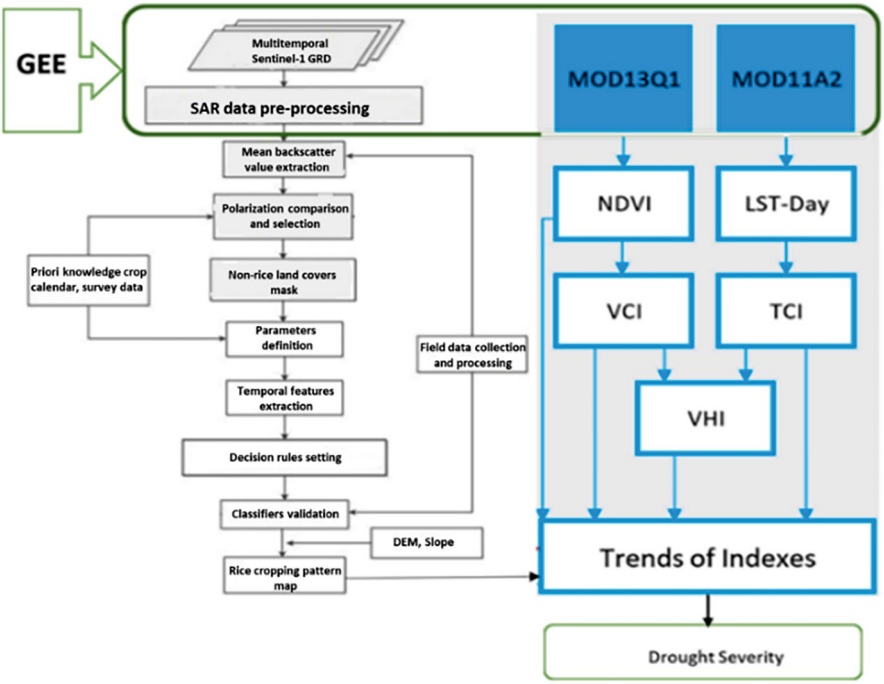

Fig. 2 The flow chart of study

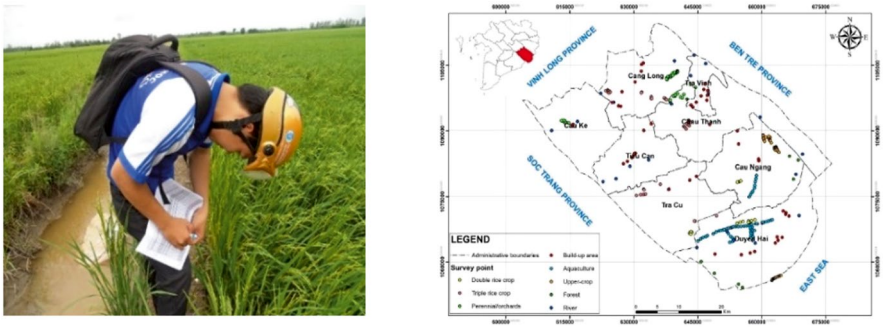

Fig. 3 Location of field survey plots throughout the study area

identified and removed non-rice elements such as seedbeds, trees, and houses, using the notes and annotations made during the field work as a guide. The spatial distribution of these digitized rice plots within the study area was then illustrated in Fig. 3. This approach helped in creating a clear and precise digital representation of the rice cultivation areas for further analysis.

Table 2 Descriptive statistics for various cropping patterns

Cropping pattern	Number of samples	Percentage
Triple rice crops	71	71%
Double rice crops-other	14	14%
Double rice crops-fallow	9	9%
Other patterns	6	6%
Total	100	100%

To evaluate how well the cropping patterns collected from field work represented the actual agricultural practices in the research region, the team conducted a comparative analysis. They compared the field data with an existing survey dataset that encompassed the same area. This involved extracting information from 60 farmers who collectively managed 100 plots within the research region. The team then summarized the observed cropping patterns in Table 2.

3.2 Polarization Comparison and Selection

Table 3 provides a detailed distribution of training and validation plots specifically for the dry season. This table breaks down the number of samples for rice, other crops, and fallow conditions. This data is vital for training and validating the models developed in this study.

The study also analyzed the backscatter dynamics of a rice plot using Sentinel-1A's VH and VV polarizations to understand their behavior during different stages of rice growth during the dry season (Fig. 4).

Our study uncovered two clearly distinguishable backscatter patterns for each polarization. Using VH polarization, we consistently observed an increase in backscatter from the beginning of the crop's growth until the reproductive period. When we examine rice using VH polarization, we observe a more consistent and predictable development pattern. On the other hand, the VV polarization showed a decrease in backscatter from the tillering to the stem elongation phases, followed by an increase during the heading stage. Rosenthal's research [15], which established a significant correlation between C-cross backscattering coefficients (VH or HV) and crop biomass/height, particularly at higher incidence angles, is consistent with the results. The observed peak backscattering values throughout the growth cycle may indicate the highest possible crop biomass. After carefully considering its capacity to accurately distinguish between land preparation and establishment phases, as well as its reliable depiction of rice growth cycles, we decided to select VH polarization for future examination. This conclusion is based on the greater dependability of accurately representing the different stages of rice growth throughout the dry season.

Table 3 Number of training and validation plots for dry season (DS)

Season	Crop/fallow	Training samples	Validation samples
DS	Rice	51	32
	Others	12	15
	Dry fallow	5	3

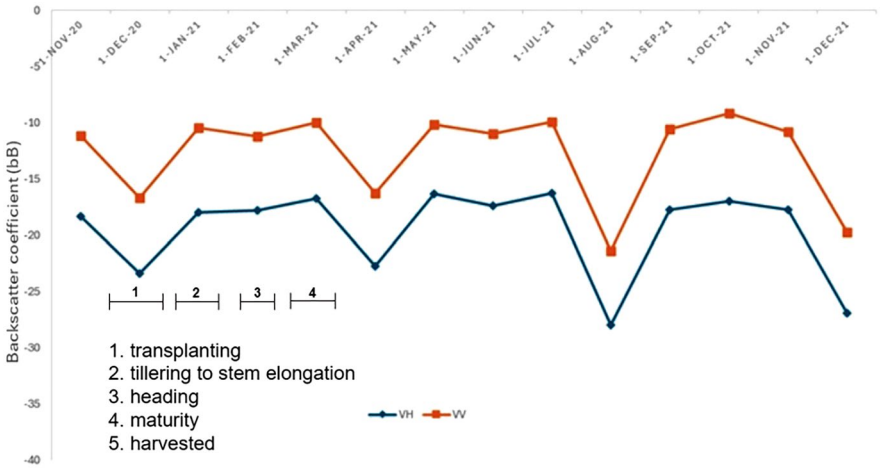

Fig. 4 Temporal changes in backscatter for a rice plot at both VH and VV polarizations

3.3 Non-rice Land Cover Mask

The research used a masking method to reduce the influence of non-rice land coverings on the categorization of rice cropping patterns. We created homogeneous sample plots on Google Earth for different land coverings, such as woods, built-up areas, and steady water. We then used the spectrum extraction program to extract the average dB values from each sample's temporal signature. For a subset of sample plots, Fig. 5 shows the backscatter dynamics of these different land coverings at VH polarization.

In Fig. 5, the backscatter dynamics are divided into two sections: dry season (DS) samples—displayed in the top section, including water bodies, built-up areas, forests, rice fields, other crops, and dry fallow land.

- Water bodies: Consistently exhibited very low to low dB values
- Urban locations (built-up): Demonstrated consistently higher backscatter
- Forests: Characterized by a constant medium to high backscatter coefficient, reflecting thick vegetation

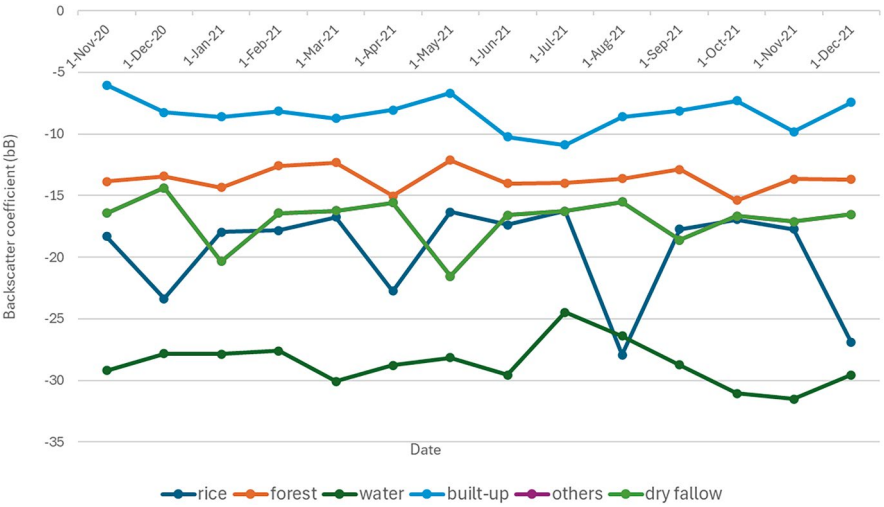

Fig. 5 VH polarization backscatter variation over time for different land cover types within selected DS sample plots

- Rice fields: Showed reduced SAR backscatter prior to crop establishment due to being typically flooded, in contrast to other crops like maize which weren't flooded during this period [16, 17]
- Dry fallow land: Displayed substantial changes in the early season with lower backscatter values in May compared to rice and other crops

Figure 5 analysis shows that water, urban, and forest areas have different backscatter characteristics over time compared to cropland and fallow land. Therefore, to accurately classify the rice cropping pattern model, the system eliminated water bodies with an average backscatter value ($\sigma\circ$) lower than -23 dB and eliminated forest and residential areas with an average $\sigma\circ$ value greater than -14 dB, based on the change in their backscatter characteristics over time throughout the year.

3.4 Satellite-Based Drought Indices

This study uses three satellite-based indices to analyze drought conditions: the Vegetation Condition Index (VCI), the Temperature Condition Index (TCI), and the Vegetation Health Index (VHI). Calculations for these indices were made possible using data from the Moderate Resolution Imaging Spectroradiometer (MODIS) sensor aboard the Terra satellite. While the 250 m resolution of MODIS might seem coarse for some applications, it is well-suited for provincial-level drought monitoring. Drought conditions generally affect large areas, and MODIS provides a broad, consistent view of vegetation health and temperature patterns across an entire province. Additionally, MODIS offers the long historical record necessary to identify

trends in drought conditions over time. Studies such as [18, 19] demonstrate successful use of MODIS for drought assessment at state and provincial levels. Calculation of Indices:

3.4.1 Vegetation Condition Index (VCI)

The VCI (Eq. 1) was used to assess the impact of weather conditions on vegetation health. We calculated VCI using 10 years of historical NDVI data derived from the MOD13Q1.006 Terra Vegetation Indices 16-Day Global 250 m dataset. VCI values helped us isolate short-term weather fluctuations from long-term ecosystem changes, revealing relative variations in moisture conditions [20].

$$\left(NDVI - NDVImin\right) / \left(NDVImax - NDVImin\right) \tag{1}$$

3.4.2 Temperature Condition Index (TCI)

The TCI (Eq. 2) was calculated using LST values to characterize drought conditions based on vegetation thermal stress. We derived LST data from the MOD11A2.006 Terra LST&E 8-Day Global 1 km dataset over a 10-year period. TCI values, in conjunction with soil moisture indicators, helped determine probabilities of drought severity [21].

$$\left(LSTmax - LST\right) / \left(LSTmax - LSTmin\right) \tag{2}$$

3.4.3 Vegetation Health Index (VHI)

To obtain a comprehensive assessment of vegetation health, we calculated the VHI (Eq. 3). VHI combines the information on moisture stress from VCI and thermal stress from TCI. Due to a lack of specific data for our study area, an equal contribution ($\alpha = 0.5$) for VCI and TCI was assumed [22].

$$\alpha \mathrm{VCI} + \left(1 - \alpha\right) \mathrm{TCI} \tag{3}$$

3.5 Image Collection Timing

The synthetic aperture radar (SAR) data used in this study was collected from the Sentinel-1 satellite. Sentinel-1 operates in a sun-synchronous orbit, which means it revisits any point on Earth every 12 days (6 days when combining Sentinel-1A and Sentinel-1B). The timing of image collection was strategically chosen to align with

the different stages of rice growth. For this study, the image series was collected from 2014 to 2021.

The MODIS images used for calculating the Vegetation Condition Index (VCI) and Temperature Condition Index (TCI) are derived from the MOD13Q1.006 Terra Vegetation Indices 16-Day Global 250 m dataset and the MOD11A2.006 Terra LST&E 8-Day Global 1 km dataset, respectively. The MOD13Q1.006 dataset provides 16-day composite images of vegetation conditions, while the MOD11A2.006 dataset provides 8-day composite images of land surface temperatures. These composite periods were selected to ensure a sufficient number of cloud-free observations at each location. MODIS images were collected from December to April of the following year for the period from 2014 to 2021. This careful selection of image collection timing is essential for accurately capturing the variations in vegetation and temperature conditions relevant to the study's objective of assessing drought conditions.

4 Result and Discussion

4.1 Map of the Rice Paddies in the Study Area

In this study, the multi-temporal backscatter coefficient ($\sigma\circ$) images were processed using a rule-based classifier to create a comprehensive rice cropping pattern map, as shown in Fig. 6.

The data from the study area revealed that there were 47,681.85 ha of triple rice crops, 11,603.29 ha of double rice crops-other, and 5025.34 ha of double rice crops-fallow. These areas account for approximately 75.4%, 18.4%, and 7.9% of the total rice-cropped area, respectively. These figures not only highlight the dominance of the triple cropping system, which takes up the majority of the agricultural land but also depict the existence of alternative double cropping practices, some of which include a fallow period (Fig. 7).

The map illustrates the spatial distribution of rice land areas, derived from a careful analysis of Sentinel-1 satellite imagery using a rule-based classification method. The accuracy of this classification was rigorously evaluated, resulting in a total accuracy of 86% and a Kappa coefficient of 0.80, indicating a high degree of reliability in the classified data. To assess the effectiveness of the method in determining rice land areas, on-site field data was compared with the classified satellite data. This comparison utilized a confusion matrix, which clarifies the differences between the observed and predicted classifications of rice land areas. Such a methodological framework proved to be indispensable for ensuring a detailed and accurate analysis of the rice land areas and cropping patterns within the research area.

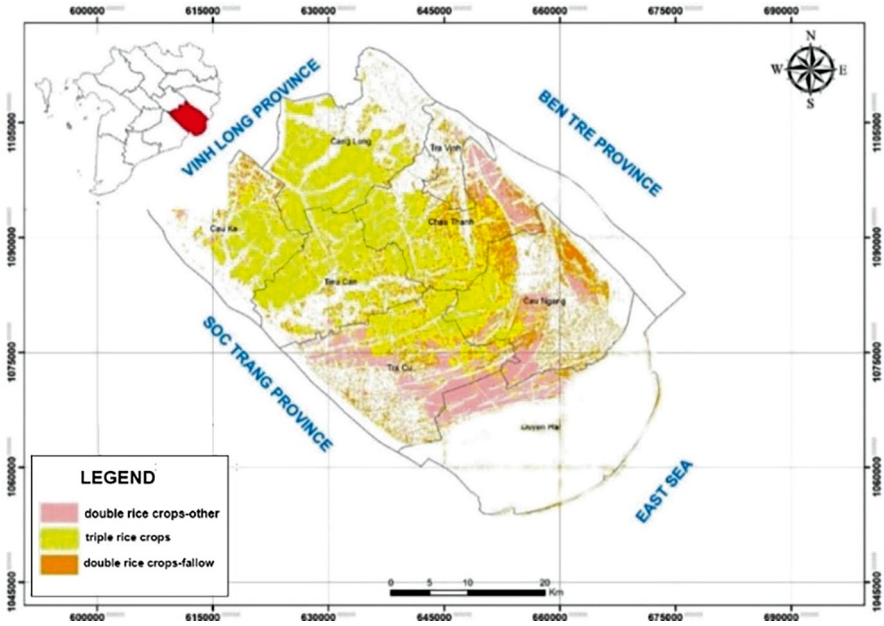

Fig. 6 Rice cropping pattern derived from rule-based classification

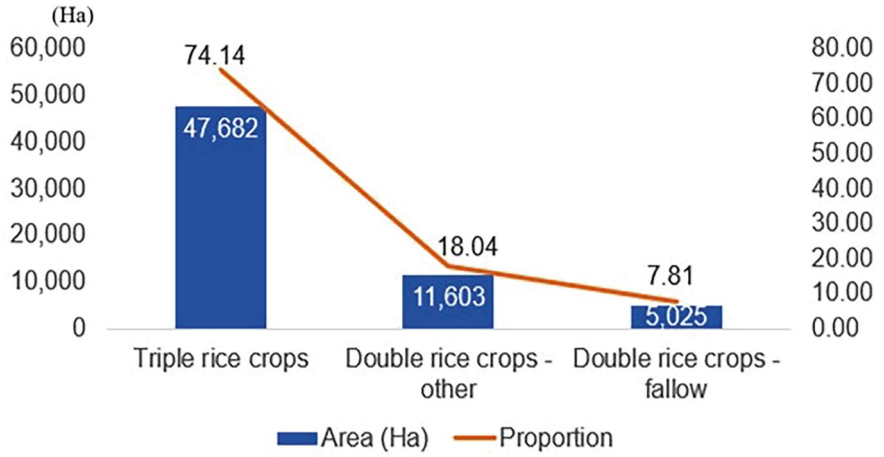

Fig. 7 Rice crop categories

4.2 Analyzing the Relationship Between Drought Intensity and Rice Yield

Figure 8 in the study, which visually depicts the Vegetation Health Index (VHI) across the study area for the period from 2014 to 2021, is crucial for highlighting the severity of drought conditions in the area. As we see in the figure, there are high areas of severe and extreme drought in the dry seasons of 2015/2016 and 2020/2021.

The comparative analysis of VHI maps over successive years reveals specific patterns in drought conditions that directly correlate to rice yields. For example, the maps from 2014 and 2015 display extensive severe drought (in red), coinciding with the periods of lowest rice yields in Fig. 9. By 2019, there is minimal drought present, and we see higher rice yields accordingly. The resurgence of drought conditions in 2020 and 2021 again corresponds with lower rice yields. This analysis further demonstrates the clear impact of drought on agricultural production.

Figure 9 directly illustrates the relationship between drought and rice yield (2014–2021). The chart depicts the relationship between different levels of drought (extreme, severe, moderate, and mild) and the corresponding rice yield (in tons per hectare). As drought intensity increases, rice yield decreases significantly. Years with extreme drought conditions, such as 2021, resulted in significantly lower rice yields. In contrast, years with milder drought exhibited higher rice yields.

4.3 Drought Trends: 2014–2021 Overviews

In the context of our preceding analysis of the relationship between drought intensity and rice yield, we now turn our attention to the trends in drought conditions from 2014 to 2021 (Fig. 10).

Our trend analysis further highlights a consistent decline in non-drought areas, decreasing from 53,144 ha in 2014 to 37,826 ha by 2021, a reduction exceeding 28%. Concurrently, there was an increase in areas experiencing moderate and mild drought, from 2888 ha to 7645 ha and from 5564 ha to 15,576 ha, respectively, over the same period. This signifies a gradual shift toward drier conditions, which, as previously established, directly correlates with decreased rice yields.

The trend graph distinctly illustrates this steady incline in areas affected by moderate and mild drought throughout the study period. Additionally, the heatmap offers a visual representation of the annual distribution of drought intensity, with progressively darker hues indicating higher severity from "No Drought" to "Extreme Drought." This visual evidence mirrors the intensification of drought conditions and the corresponding decrease in rice yield over the years.

The integration of these two visual tools not only illuminates interannual variability but also underscores the long-term aridification trend. This trend could have profound implications for water resource management and agricultural planning, considering the established impact of drought on rice yield.

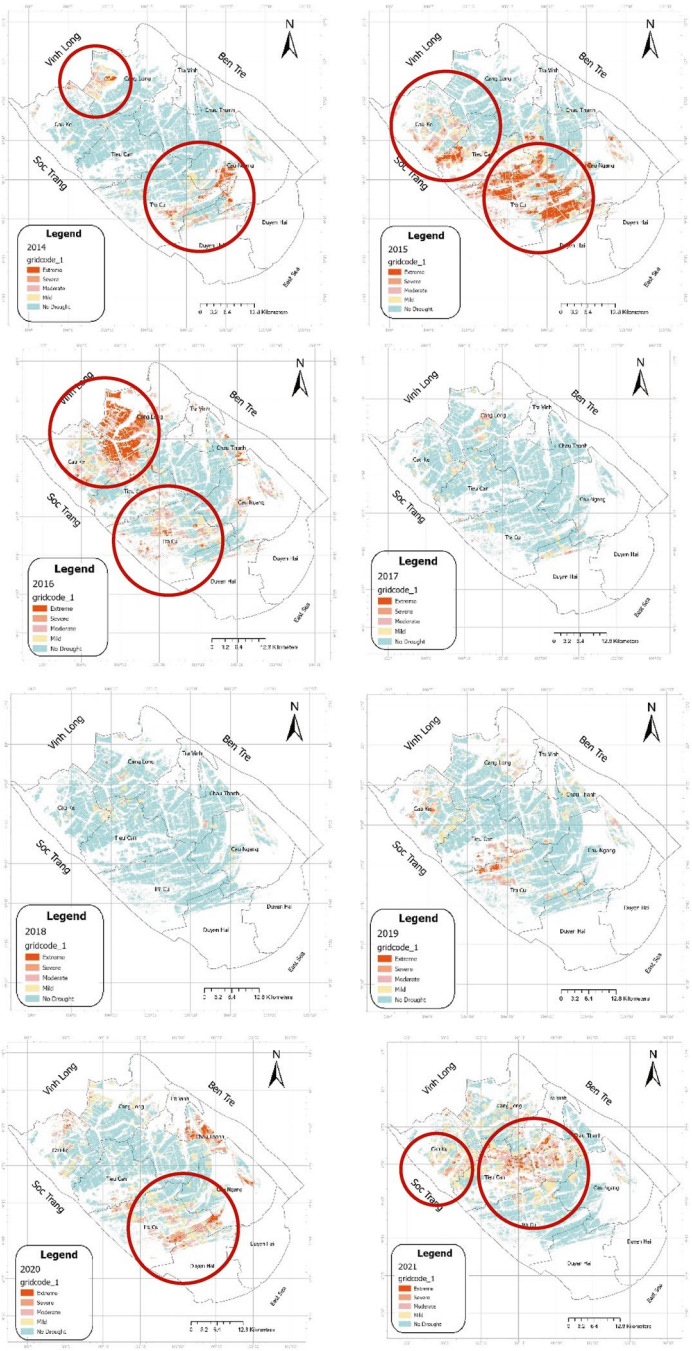

Fig. 8 VHI depicts high areas of severe and extreme drought in dry seasons of 2015/2016 and 2020/2021

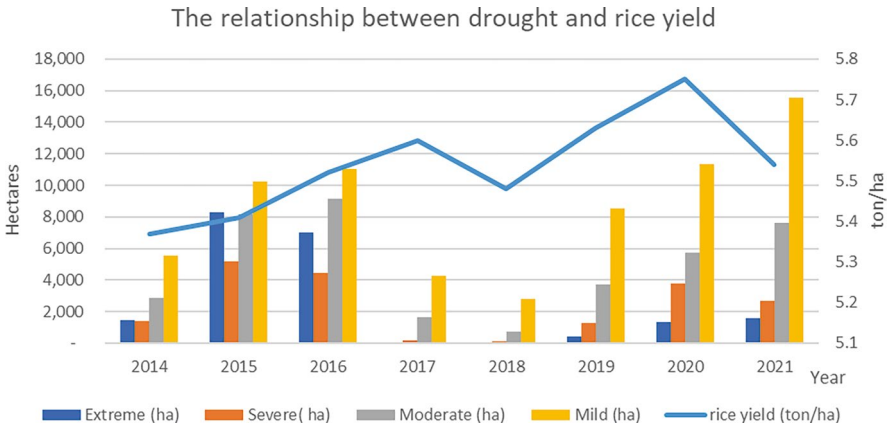

Fig. 9 The relationship between drought and rice yield (2014–2021)

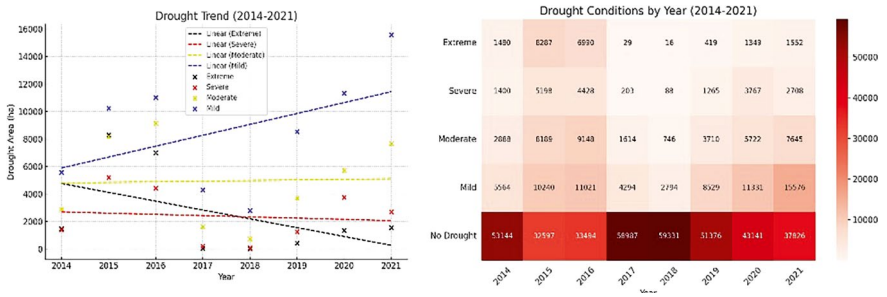

Fig. 10 Drought severity trends and distribution, 2014–2021

In summarizing these trends, the complex and evolving patterns of drought are starkly depicted. While individual years may present significant deviations, the overarching trend points toward an increasingly arid future in line with climate change forecasts. These insights emphasize the urgent need for comprehensive strategies to mitigate the impacts of drought on rice yield and adapt to an ever-changing climatic landscape.

4.4 Achievements, Limitations, and Scope of Results

Achievements: This study successfully demonstrates the combined utility of Sentinel-1 satellite data and the Vegetation Health Index (VHI) for mapping rice cropping patterns and assessing the spatio-temporal dynamics of drought in a major rice-producing region. The rule-based classifier achieved reasonable accuracy, and the VHI effectively captured drought severity and fluctuations over time.

Limitations: While our methodology offers valuable insights, it is important to acknowledge its limitations. The rule-based classifier, though effective, may encounter challenges in areas with complex cropping systems or mixed land use patterns. Additionally, the VHI, while sensitive to vegetation stress, could be influenced by factors other than drought, such as disease or nutrient deficiency.

Scope of results: The findings of this study have significant implications for agricultural planning and drought mitigation in the region. By providing detailed information on rice cropping patterns and drought trends, decision-makers can develop targeted interventions to enhance crop resilience and water resource management. Moreover, the methodology developed in this study has the potential to be adapted for monitoring agricultural systems in other regions facing climate change challenges.

Future directions: Building on the present work, future research could explore the integration of multi-sensor data sources to improve classification accuracy. Furthermore, incorporating ground-based data and crop models could enhance the understanding of the complex interactions between drought, crop yields, and other environmental factors.

5 Conclusion

This study successfully demonstrated the effectiveness of combining Sentinel-1 satellite data and the Vegetation Health Index (VHI) to map rice cultivation patterns and assess drought conditions in Tra Vinh province, Vietnam. By utilizing Google Earth Engine and analyzing multi-temporal SAR data, we accurately classified different rice cropping systems in the region. The VHI derived from MODIS data proved valuable in analyzing the spatio-temporal patterns of drought conditions from 2014 to 2021.

The study has brought forth several key findings. The first is the dominance of triple rice cropping, which occupies about 75% of the total rice cultivation area. The second is a significant interannual variability in drought severity, with particularly severe conditions observed in 2015 and a resurgence in 2020/2021. This points toward a concerning trend of increasing areas affected by mild and moderate drought conditions. Lastly, the study underscores the importance of remote sensing techniques, particularly SAR data, for monitoring agricultural systems in tropical regions with frequent cloud cover.

These findings have substantial implications for sustainable agricultural planning and water resource management in Tra Vinh province and similar rice-producing regions. The detailed data on rice cropping patterns and drought dynamics can guide targeted interventions to enhance crop resilience, optimize water usage, and mitigate climate change impacts.

Future research could aim at integrating multi-sensor data sources for better accuracy in rice crop classification and drought assessment. Also, ground-based

measurements and crop models could be employed to better understand the complex relationships between drought, crop yields, and other environmental factors.

In conclusion, this study offers essential tools and insights that can aid policymakers and agricultural practitioners in formulating effective strategies to tackle the challenges posed by drought and ensure long-term food security.

Acknowledgments We would like to express our gratitude to VNU-HCM for the funding provided under grant C2023-16-14.

References

1. General Statistics Office of Vietnam (GSO). https://www.gso.gov.vn/default_en.aspx?tabid=778
2. Mirzapour, S., Karimi, S., Zarkesh, M.K., et al.: Mapping the spatial distribution of Rice fields in southern coast of Caspian Sea using Landsat 8 time-series images. J Geography Nat Disasters. **08**(1) (2018). https://doi.org/10.4172/2167-0587.1000215
3. Huang, C., Yang, Q., Guo, Y., et al.: The pattern, change and driven factors of vegetation cover in the Qin Mountains region. Sci. Rep. **10**, 1–11 (2020). https://doi.org/10.1038/s41598-020-75845-5
4. Kukunuri, A.N.J., Murugan, D., Singh, D.: Variance based fusion of VCI and TCI for classification of agriculture drought using MODIS data. Geocarto Int. **37**, 1–22 (2020). https://doi.org/10.1080/10106049.2020.1837256
5. Liu, Z., Liu, H., Luo, C., et al.: Rapid extraction of regional-scale agricultural disasters by the standardized monitoring model based on Google Earth Engine. Sustain. For. **12**, 6497 (2020). https://doi.org/10.3390/su12166497
6. Dong, J., Xiao, X., Menarguez, M.A., et al.: Mapping paddy rice planting area in northeastern Asia with Landsat 8 images, phenology-based algorithm and Google earth engine. Remote Sens. Environ. **185**, 142–154 (2016). https://doi.org/10.1016/j.rse.2016.02.016
7. Raksapatcharawong, M., Veerakachen, W., Homma, K., et al.: Satellite-based drought impact assessment on Rice yield in Thailand with SIMRIW−RS. Remote Sens. **12**, 2099 (2020). https://doi.org/10.3390/rs12132099
8. Xinghua, L., Huanfeng, S., Liangpei, Z., et al.: Recovering quantitative remote sensing products contaminated by thick clouds and shadows using multitemporal dictionary learning. IEEE Trans. Geosci. Remote Sens. **52**, 7086–7098 (2014)
9. Li, X., Wang, L., Cheng, Q., et al.: Cloud removal in remote sensing images using nonnegative matrix factorization and error correction. ISPRS J. Photogramm. Remote Sens. **148**, 103–113 (2019)
10. Lee, K.Y., Sim, J.Y.: Cloud removal of satellite images using convolutional neural network with reliable cloudy image synthesis model. In: Proceedings of the International Conference on Image Processing, ICIP, Taipei, Taiwan, 22–25 September 2019, pp. 3581–3585
11. Minh, H.V.T., Avtar, R., Mohan, G., et al.: Monitoring and mapping of rice cropping pattern in flooding area in the Vietnamese Mekong Delta using sentinel-1A data: a case of An Giang province. ISPRS Int. J. Geo Inf. **8**, 211 (2019)
12. Phung, H.P., Nguyen, L.D.: Rice crop monitoring in the Mekong Delta, Vietnam using multi-temporal Sentinel-1 data with C-band. In: Reddy, J.N., Wang, C.M., Luong, V.H., Le, A.T. (eds.) ICSCEA 2019, Lecture Notes in Civil Engineering 80, pp. 979–986. Springer Nature Singapore Pte Ltd., Berlin/Heidelberg, Germany (2020) ISBN 9789811551437
13. People's Committee of Tra Vinh Province: Introduction. https://travinh.gov.vn/gioi-thieu

14. Rosenthal, W., Blanchard, B., Blanchard, A.: Visible/infrared/microwave agriculture classification, biomass, and plant height algorithms. IEEE Trans. Geosci. Remote Sens. **GE-23**(2), 84–90 (1985). https://doi.org/10.1109/TGRS.1985.289404
15. GSO: General Statistics Office of Vietnam. https://www.gso.gov.vn/default_en.aspx?tabid=778. Accessed 4 Mar 2020
16. Asilo, S., de Bie, K., Skidmore, A., et al.: Complementarity of two rice mapping approaches: characterizing strata mapped by hypertemporal MODIS and rice paddy identification using multitemporal SAR. Remote Sens. **6**(12), 12789–12814 (2014). https://doi.org/10.3390/rs61212789
17. Boschetti, M., Nutini, F., Manfron, G., et al.: Comparative analysis of normalized difference spectral indices derived from MODIS for detecting surface water in flooded rice cropping systems. PLoS One. **9**(2), e88741 (2014)
18. Kogan, F.N., et al.: A drought monitoring system for the state of California using MODIS and SPOT data. Remote Sens. Environ. **86**(5), 576–588 (2003)
19. Venkatesh, N., et al.: Drought monitoring and assessment in Karnataka state, India, using MODIS data. Int. J. Remote Sens. **31**(10), 2729–2743 (2010)
20. Kogan, F., Gitelson, A., Zakarin, E., Spivak, L., Lebed, L.: AVHRR-based spectral vegetation index for quantitative assessment of vegetation state and productivity: calibration and validation. Photogramm. Eng. Remote Sens. **69**(8), 899–906 (2003). https://doi.org/10.14358/PERS.69.8.899
21. Unganai, L.S., Kogan, F.N.: Drought monitoring and corn yield estimation in southern Africa from AVHRR data. Remote Sens. Environ. **4257**, 219–232 (1998). https://doi.org/10.1016/S0034-4257(97)00132-6
22. Sun, B., Qian, J., Chen, X., Zhou, Q.: Comparison and evaluation of remote sensing indices for agricultural drought monitoring over kazakhstan. Int. Arch. Photogramm. Remote Sens. Spatial Inf. Sci. **XLIII-B3-2020**, 899–903 (2020). https://doi.org/10.5194/isprs-archives-XLIII-B3-2020-899-2020